Tu B3 06

Practical Benefits of Kirchhoff Least-squares Migration Deconvolution

L. Casasanta* (CGG), G. Roberts (CGG), F. Perrone (CGG), A. Ratcliffe (CGG), G. Poole (CGG), Y. Wang (CGG), Y. Xie (CGG)

Summary

Kirchhoff images can suffer from uneven illumination and contamination by migration artefacts, particularly in regions of more complex geology. One issue is that migration is not a true inverse operation – it is based on the adjoint of the forward modelling operator. In contrast, least-squares migration approximates the inverse of the forward modelling and, with a sufficiently accurate velocity model, the impact of the detrimental effects on the image can be reduced. Here, we describe the benefits of a non-iterative Kirchhoff least-squares method, usually referred to as migration deconvolution. We present a practical workflow to demonstrate that the method can be used to attenuate image artefacts, particularly the strong wave-front swings, to help balance image illumination, and increase clarity and robustness of AVO attributes. We illustrate our workflow on a real data example from offshore Gabon, in which we are careful to ensure that both the conventional and migration deconvolution have the same pre-processing sequence applied prior to imaging. This sequence includes elements (de-ghosting, spectral balancing, regularization and interpolation) designed to improve the quality of the conventional Kirchhoff image, as well as de-multiple and de-noise processing. We observe a distinct, yet realistic, uplift from the migration deconvolution over conventional migration.

Introduction

Seismic depth migration is the process in which reflection events recorded at the surface are re-positioned to the locations where the events occurred in the subsurface. In an ideal world this will create an image that represents the subsurface geological structure and reflectivity. However, this image is often contaminated with artefacts. Huang et al. (2014) highlight the problems of: (1) under-sampled and irregular acquisition geometry; (2) areas of poor resolution resulting from limited recording aperture; (3) ringing artefacts caused by ripples in the source wavelet, and (4) weak amplitudes resulting from geometrical spreading, attenuation and defocusing. Some of these problems can be handled as part of a good pre-processing sequence, but there remains the underlying issue that the migration operator is not the inverse of the forward single-scattering modelling operation – it is in fact its adjoint. In contrast, least-squares migration is a formal (least-squares) inversion of the forward modelling operator, such that, with a sufficiently accurate velocity model, the impact of the artefacts from conventional imaging can be reduced. Because of its large dimensionality – namely millions of seismic data points multiplied by millions of reflectivity traces – the migration inverse problem is often solved using an iterative, gradient-based, approach. A more efficient method is to solve the normal equations by computing the Hessian matrix either directly using point-spread-functions (Fletcher et al., 2015) or indirectly using non-stationary matching filters (Guitton, 2004). These methods reduce the computational cost to approximately a single iteration of the iterative schemes. Therefore, in recent years there has been increased interest in what we describe as single iteration, or non-iterative, least-squares imaging methods. In the context of common-offset Kirchhoff migration, we demonstrate with synthetic and real data examples that a non-iterative least-squares method attenuates image artefacts, improves illumination and acts as a de-noise/image enhancement on AVO attribute sections, particularly in regions around faults.

Method

Conceptually, Kirchhoff seismic modelling (or de-migration) can be written as a linear problem

$$d = Lr\,, \tag{1}$$

where d are observed seismic data, r are subsurface reflectivity traces and L is the Kirchhoff modelling operator. Ideally, to compute subsurface reflectivity we would solve the inverse problem

$$r = L^{-1}d\,. \tag{2}$$

In real world situations (discrete, finite-aperture acquisition; incomplete subsurface illumination), computation of the direct inverse is not feasible, and the common alternative is to use the adjoint of L

$$m = L^{T}d\,, \tag{3}$$

where m is the Kirchhoff migrated image, which can suffer from artefacts and illumination issues. To mitigate these effects Nemeth et al. (1999) developed a formulation that updates the migrated image by matching the observed data with modelled (de-migrated) data by minimising a least-squares cost function, $f(r) = \| d - Lr \|^2$. The least-squares solution is obtained by solving the normal equations:

$$r = \left(L^{T}L\right)^{-1}L^{T}d\,, \tag{4}$$

where $L^{T}L$ is usually referred to as the Hessian operator. Equation (4) can be solved iteratively using, for example, steepest descent or conjugate gradient methods. However, we observe that substituting the migration image (3) into equation (4) gives

$$r = \left(L^{T}L\right)^{-1}m\,. \tag{5}$$

Hence, if we can estimate the Hessian matrix directly we can apply it to the initial migration to reduce the artefacts in this migration. To do this, we follow an approach similar to Guitton (2004), using non-stationary matching filters to estimate the Hessian. This approach has been further developed by both Khalil et al. (2016) and Wang et al. (2016). We follow their implementations with a flow of: initial migration, de-migration, and subsequent re-migration. The Hessian is estimated by matching the initial migration with the corresponding re-migration. The matching of the images is carried out using curvelet domain filters that bring stability and structural consistency to the process (Wang et al., 2016). This scheme is a type of image-domain migration deconvolution (Hu et al., 2001). It is robust, non-iterative and, consequently, more cost effective than the traditional iterative approach.

Synthetic data example

Two of the key benefits of migration deconvolution are attenuation of migration swing artefacts and improved illumination. Swing artefacts are often seen in Kirchhoff images, and their clean removal generally proves to be very resistant to signal processing methods. We now demonstrate the above benefits with a simple positive Gaussian anomaly 3D synthetic example.

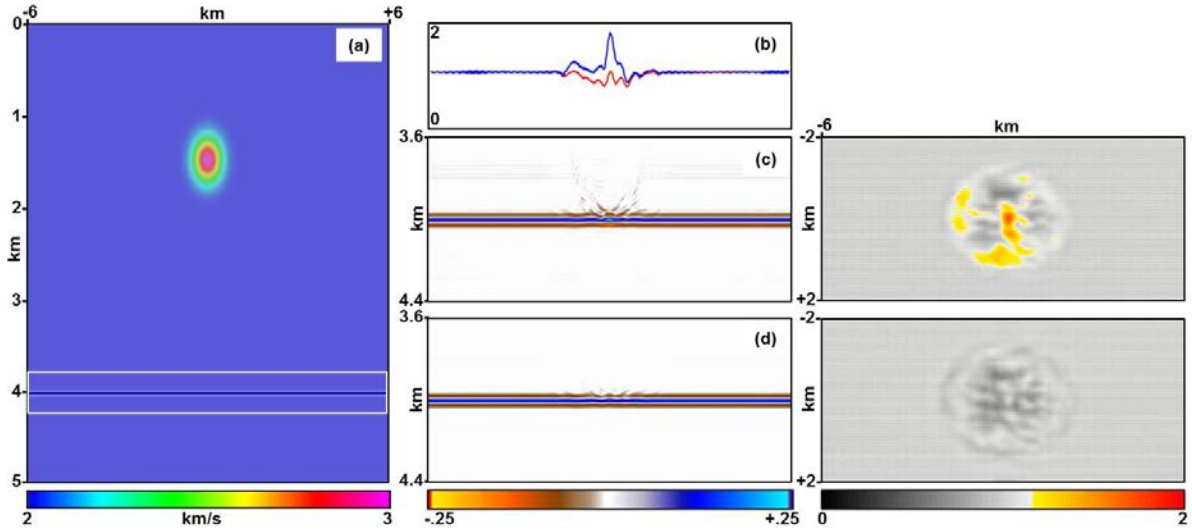

Figure 1 *(a) Extracted single central line from the positive Gaussian anomaly velocity model with a deeper target reflector highlighted in the white box. (b) Single central line extraction of normalised rms amplitudes of the reflector for images of conventional Kirchhoff migration (in blue) and migration deconvolution (in red). Single central line image: (c) after conventional Kirchhoff migration, and (d) after migration deconvolution. Depth slice at reflector of normalised rms amplitudes: (e) after conventional Kirchhoff migration, and (f) after migration deconvolution.*

In Figure 1a we show the central section of the full 3D velocity model that contains a positive 3 km/s Gaussian anomaly in a constant 2 km/s background. This anomaly is located at a depth of 1.5 km, with a constant, band-limited (18 Hz Ricker) wavelet, and a reflecting horizon at 4 km depth. We model a 565 m constant offset data volume using the shot and receiver geometry locations extracted from a real narrow-azimuth offshore acquisition (described in the next section). The conventional Kirchhoff migrated image (Figure 1c) displays the expected uneven illumination at the reflector depth where the illumination imprint caused by the anomaly gives a high amplitude peak with strong migration swings. The reflector amplitudes are more balanced and the migration swings are attenuated after application of migration deconvolution (Figure 1d). To highlight the improved amplitude balancing, normalised rms amplitude trends along the reflectors before (blue) and after (red) migration deconvolution are plotted in Figure 1b. Also, depth slices at the reflector level of normalised rms amplitudes show a more uniform amplitude distribution after migration deconvolution (Figure 1f) compared to the conventional migration (Figure 1e), which has higher amplitudes due to uneven illumination in the zone below the anomaly. However, we still observe some subtle amplitude variations in these results – these are likely due to the compromise between the large curvelet domain analysis window needed for a stable deconvolution and the small window needed to better honour local variations in the inverse Hessian. Nevertheless, this 3D synthetic demonstrates that migration deconvolution balances uneven illumination and attenuates migration swings.

Offshore Gabon data example

We now apply migration deconvolution to data from a 3D marine seismic survey acquired over the deep-water part of the South Gabon Basin. The survey was acquired using a variable-depth streamer configuration for low-noise, broad-bandwidth data (Soubaras and Dowle, 2010). Kirchhoff depth migration provided detailed structural images; however, the presence of salt bodies resulted in cross-

cutting swing artefacts and uneven illumination in some locations. In Figure 2a we show a Kirchhoff image from offset 565 m where close-to-vertical swings cut across over-thrust carbonate slabs to reduce event coherency. These are shown in the greyscale zooms of A and B in Figure 2c. We also highlight some areas of reduced illumination in the Kirchhoff image (arrows), as well as in zoom C which shows the pre-salt structures where the target sands are located. In the Kirchhoff image this pre-salt region is characterized by speckled noise and reduced event coherency. In Figure 2b we show that migration deconvolution reduces the swing artefacts (zooms A and B in Figure 2d) and generally boosts illumination in the deeper section. Also, comparing zoom C in Figures 2c and 2d shows noise reduction and improved event coherency after migration deconvolution. Both Kirchhoff images have exactly the same pre-processing sequence, with that sequence including all of the standard elements (de-ghosting, spectral balancing, regularisation and interpolation) that are designed to improve the quality of the conventional Kirchhoff image, as well as the usual de-multiple and de-noise steps.

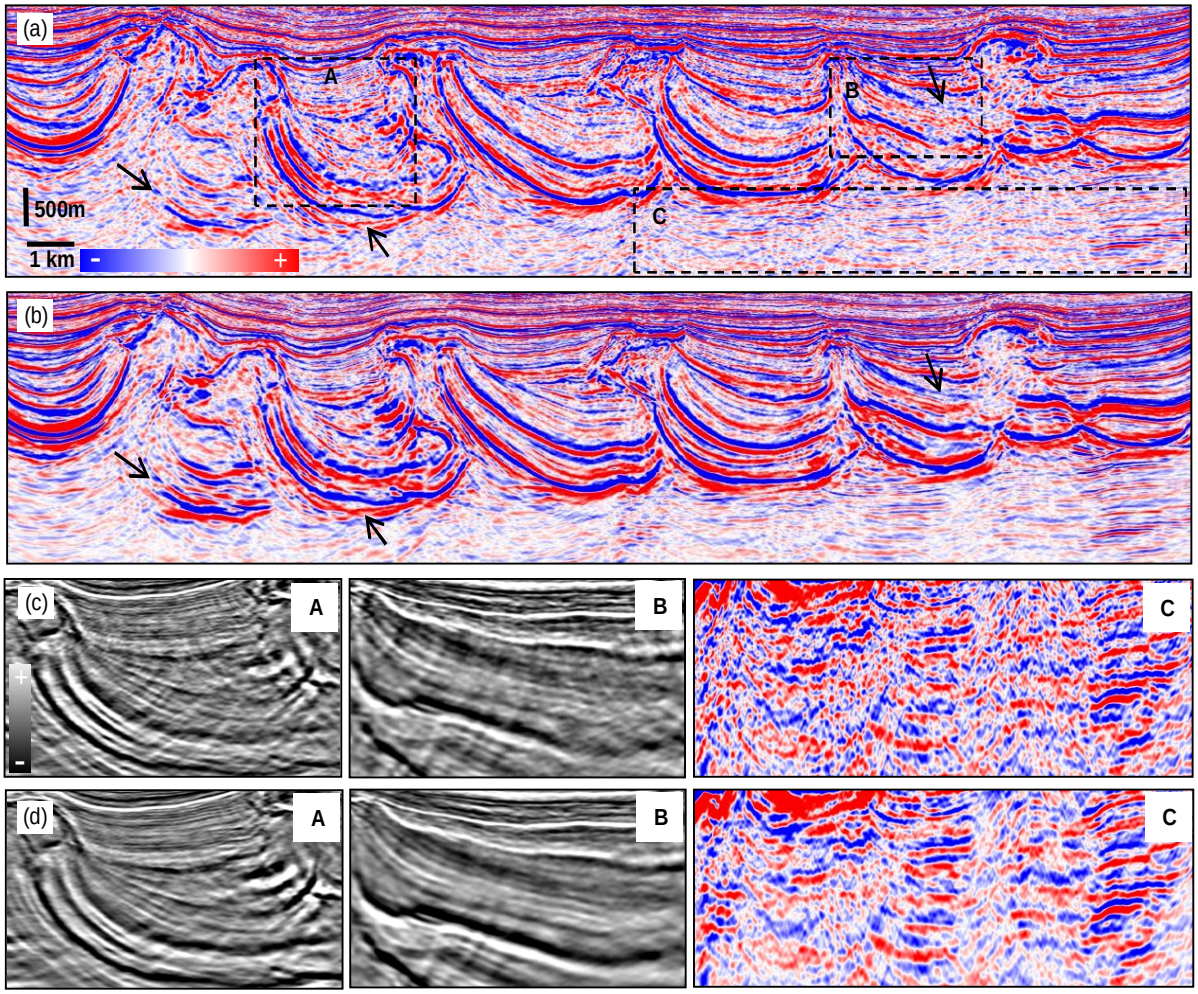

Figure 2 *(a) Conventional Kirchhoff image (offset 565 m); (b) migration deconvolution (offset 565 m); (c) Zooms A, B and C for conventional Kirchhoff image and (d) Zooms A, B and C for migration deconvolution. Zooms A and B highlight migration swing noise attenuation and zoom C highlights noise reduction and event continuity in the deeper pre-salt region.*

The application of migration deconvolution can also improve the quality of inverted AVO attributes. The AVO gradient, in particular, is sensitive to noise and uneven illumination across offsets. In Figure 3a we show the AVO gradient estimated from a conventional Kirchhoff migration which has poor event coherency – this is particularly noticeable in the fault zones (lower ellipse) and in the shallow sand channels (upper ellipse). In Figure 3b we show that migration deconvolution improves the AVO gradient event coherency, sharpens the structure of the sand channels, and improves fault definition.

Conclusions

We have described a non-iterative least-squares Kirchhoff migration and its application to both synthetic and real data. The method is formulated as an image-domain migration deconvolution using non-stationary matching filters in the curvelet domain. The method proves to be stable, robust, and efficient. The synthetic data example demonstrated that the method can mitigate uneven illumination effects and reduce migration swing artefacts that are generally difficult to remove post-migration. This was confirmed in the real data example from offshore Gabon where we clearly observe the attenuation of migration artefacts, especially the close-to-vertical salt swings, and improved illumination. The AVO gradient, which is particularly sensitive to noise and uneven illumination across offsets, shows considerable uplift after migration deconvolution.

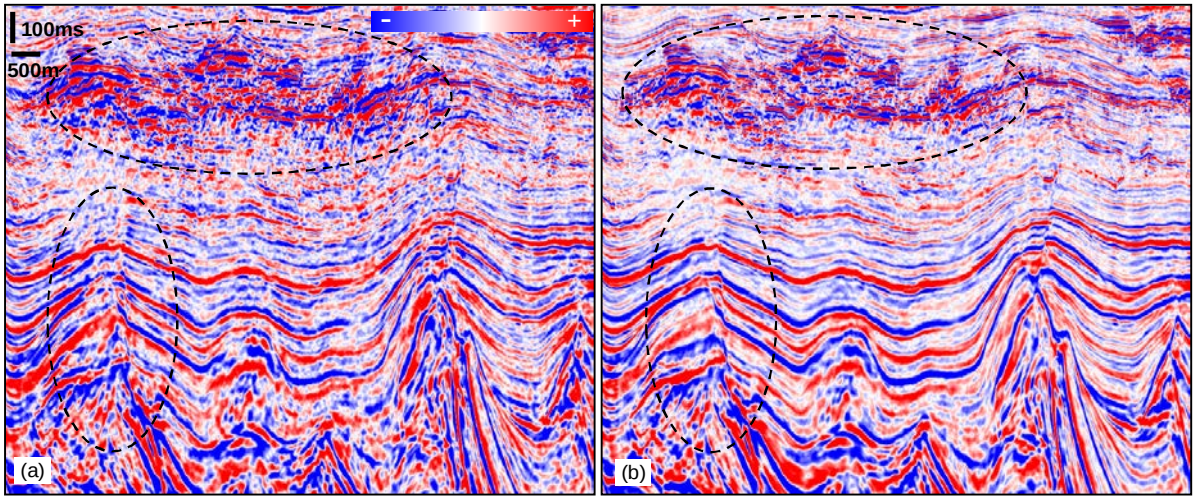

Figure 3 *Estimated AVO gradient: (a) before, and (b) after migration deconvolution.*

Acknowledgements

We thank CGG for permission to publish this work and CGG's Multi-Client & New Ventures business line for permission to show the real data example. We also thank Adel Khalil whose research motivated this work and Steve Thompson for geological input.

References

Fletcher, R.P., Nichols, D., Bloor, R.M. and Coates, R.T. [2015] Least-squares migration: data domain versus image domain. *77th EAGE Conference & Exhibitions*, Extended Abstracts, We N106 06.

Guitton, A. [2004] Amplitude and kinematic corrections of migrated images for non-unitary imaging operators. *Geophysics*, **69**, 1017–1024.

Hu, J., Schuster G., and Valasek P. A. [2001] Poststack migration deconvolution. *Geophysics*, **66** (3), 939-952.

Huang, Y., Dutta, G., Dai, W., Wang, X., Schuster, G.T. and Yu, J. [2014] Making the most out of least-squares migration. *The Leading Edge*, **33** (9), 954-960.

Khalil, A., Hoeber, H., Roberts, G. and Perrone, F. [2016] An alternative to least-squares imaging using data-domain matching filters. *86th Annual International Meeting*, SEG, Expanded Abstracts, 4188-4192.

Nemeth, T., Wu, C. and Schuster, G.T. [1999] Least-squares migration of incomplete reflection data. *Geophysics*, **64** (1), 208-221.

Soubaras, R., and R. Dowle [2010] Variable-depth streamer – a broadband marine solution. *First Break*, **28** (12), 89–96.

Wang, P., Gomes, A., Zhang, Z. and Wang, M. [2016] Least-squares RTM: Reality and possibilities for subsalt imaging. *86th Annual International Meeting*, SEG, Expanded Abstracts, 4204-4209.